

Reservoir computing using consistency of semiconductor lasers with optical feedback and injection

Joma Nakayama¹, Kazutaka Kanno^{1,2}, and Atsushi Uchida¹

¹Department of Information and Computer Sciences, Saitama University,
 255 Shimo-Okubo, Sakura-ku, Saitama City, Saitama, 338-8570, Japan

²Department of Electronics Engineering and Computer Science, Fukuoka University,
 8-19-1 Nanakuma, Johnan-ku, Fukuoka 814-0180, Japan

Emails: s14mm327@mail.saitama-u.ac.jp, kkanno@fukuoka-u.ac.jp, auchida@mail.saitama-u.ac.jp

Abstract—Reservoir computing is a novel bio-inspired computing method and highly efficient approach for processing empirical data. One of the important properties of reservoir computing is consistency, where the same response output can be observed by a repeated drive signal. Semiconductor lasers with optical injection show consistent outputs. We implement reservoir computing by using semiconductor lasers subject to optical delayed-feedback and injection. We investigate the performance on Santa Fe laser time-series prediction task.

1. Introduction

Reservoir computing is a novel computing method inspired by the human brain [1-3]. Reservoir computing can solve some tasks (e.g. time-series prediction and speech recognition) using machine learning with training data and output weights. In 2011, a method using a nonlinear dynamical system subject to delayed-feedback has been demonstrated [4]. Since then, many studies on reservoir computing with optical dynamical systems have been reported intensively to achieve high-speed processing [5-10].

One of the important characteristics for reservoir computing is consistency. Consistency is defined as the reproducibility of the response output driven repeatedly by a complex signal, as shown in Fig. 1. Consistency has been observed in laser systems [11]. To achieve consistency, transient dynamics at a steady state has been mainly used in reservoir computing [4,5,7,8]. Recently, optical injection of a constant drive signal to a semiconductor laser has been used to obtain consistent response output [9,10]. However, no studies have been reported by using consistency of a semiconductor laser with respect to a chaotic drive signal. A chaotic drive signal may enhance the performance of reservoir computing.

In this paper, we introduce a scheme for reservoir computing using semiconductor lasers with optical feedback and injection. We perform a time-series prediction task with the semiconductor laser systems. We used both constant and chaotic drive signals to test the performance of the prediction task.

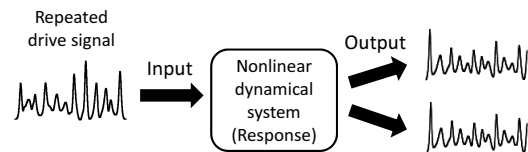


Figure 1: Concept of consistency.

2. Model of Reservoir computing

We use a scheme for reservoir computing using a semiconductor laser with optical injection, as shown in Fig. 2. For pre-processing, temporal mask is applied for each input data. The input data is expanded for the time duration T . The temporal mask consists of a piecewise constant function with a randomly-modulated binary sequence $\{-1, 1\}$ with equal probabilities. The length of the temporal mask matches the length of the input time duration T . This interval is divided into N sub-intervals of node separation θ , where $T = N\theta$. The input signal is constructed by the convolution of the input data with the temporal mask.

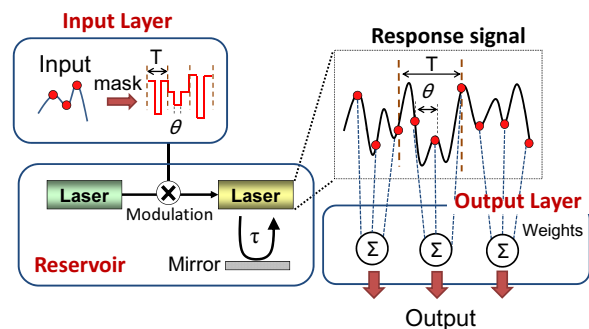


Figure 2: Schematics of reservoir computing.

For post-processing, virtual nodes x_i ($i = 1, 2, \dots, N$) are defined as the outputs of the response laser in the feedback loop at the final point of each interval θ . A linear combination of the output of the virtual nodes $x_i(n)$ with weights W_i is calculated for machine learning, where $y(n) = \sum_i W_i x_i(n)$ for n -th input data. The weights are optimized by training process. The weighted output $y(n)$ is used to evaluate the performance of reservoir computing.

There are two approaches to determine the input time

duration T . The input time T can be set to be exactly the same as the feedback delay time $\tau = T$, known as the synchronized scheme [4, 5, 8, 9, 10]. On the contrary, the input time T can be slightly mismatched to the feedback delay time $\tau = T + \theta$, known as the unsynchronized scheme [6, 7]. We used the unsynchronized scheme since the mismatch between T and τ results in rich variation of the nodes and good performance of reservoir computing [6, 7].

We set the parameter values for our numerical simulations as follows: $\theta = 0.1$ ns, $N = 400$, $T = 40.0$ ns, and $\tau = 40.1$ ns.

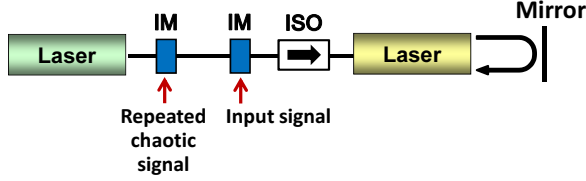


Figure 3: Schematics of reservoir using two semiconductor lasers with optical feedback and injection. IM, intensity modulator. ISO, optical isolator.

Figure 3 shows the schematics of the reservoir with unidirectionally-coupled two semiconductor lasers. The optical output of one semiconductor laser (called drive laser) is injected into the other laser (called response laser). The response laser has an external mirror to add time-delayed optical feedback. The outputs in the time-delayed feedback loop are used as the nodes for reservoir computing. The intensity of the drive laser output is modulated by the input signal. For one case, the drive laser is set to a constant output without the input signal, as used in Refs. [9, 10]. For the other case, we consider an additional modulation of the drive signal by using a pre-recorded chaotic temporal waveform. A chaotic signal is prepared from a semiconductor laser with optical feedback and recorded in a memory. A segment of the chaotic signal is selected with the length of the input time duration T . The intensity of the drive signal is repeatedly modulated by using the finite-length chaotic signal and sent to the response laser so that consistent output can be observed with respect to each repetition of the chaotic signal. We expect that chaos modulation of the drive signal may result in a variety of node dynamics and may enhance the performance of reservoir computing. Note that it is important to maintain the consistency of the response laser outputs even when the chaotic signal of the drive laser is injected into the response laser [11].

We implement reservoir computing using consistency of a semiconductor laser with optical feedback and injection in numerical simulations. The dynamics of semiconductor lasers is calculated by using Lang-Kobayashi equations as follows [12].

$$\frac{dE_r(t)}{dt} = \frac{1 + i\alpha}{2} \left\{ \frac{G_N(N(t) - N_0)}{1 + \varepsilon |E(t)|^2} - \frac{1}{\tau_p} \right\} E(t)$$

$$+ \kappa E_r(t - \tau) \exp(-i\omega_r \tau) + \kappa_{inj} E_d(t) \exp(i\Delta\omega t) + \xi(t) \quad (1)$$

$$\frac{dN_r(t)}{dt} = J - \frac{N_r(t)}{\tau_s} - \frac{G_N(N_r(t) - N_0)}{1 + \varepsilon |E_r(t)|^2} |E_r(t)|^2 \quad (2)$$

where $E_d(t)$ and $E_r(t)$ are the electric field amplitudes of the drive and response lasers, and $N_r(t)$ is the carrier density of the response laser. α is the linewidth enhancement factor, G_N is the gain coefficient, N_0 is the carrier density at transparency, ε is the saturation coefficient, $\tau_{p,s}$ are the photon and carrier lifetimes, κ is the feedback strength of the response laser, κ_{inj} is the injection strength from the drive to response laser. $\omega_{d,r}$ are the optical angular frequency of the drive and response lasers. $j_{d,r}$ are the injection currents normalized by the lasing threshold. J_{th} is the injection current at lasing threshold. $\Delta\omega$ is the angular frequency detuning ($2\pi\Delta f$). τ is the feedback delay time of the response laser. These parameter values are summarized in Table 1. We added the white Gaussian noise $\xi(t)$ to the electric field. The signal-to-noise ratio is set to -20 dB in our numerical simulations.

Table 1: Laser parameter values used in numerical simulations

Parameter	Value
α	3.0
G_N	$8.40 \times 10^{-13} \text{ m}^3 \text{ s}^{-1}$
N_0	$1.40 \times 10^{24} \text{ m}^{-3}$
ε	2.0×10^{-23}
τ_p	$1.927 \times 10^{-12} \text{ s}$
τ_s	$2.04 \times 10^{-9} \text{ s}$
κ	74.55 ns^{-1}
κ_{inj}	155.32 ns^{-1}
ω_d	$1.23 \times 10^{15} \text{ rad/s}$
$\Delta f (= \Delta\omega/2\pi = (\omega_d - \omega_r)/2\pi)$	0.0 GHz
τ	40.0 ns
$j_d (= J_d/J_{th})$	1.30
$j_r (= J_r/J_{th})$	1.05

2.1. Performance of Santa Fe time-series prediction task

To evaluate the performance of our scheme, we used the Santa Fe time-series prediction task [13]. The aim of the task is to predict one step ahead of chaotic data generated from a far-infrared laser. The input chaotic data and the predicted data are compared for the evaluation of the performance. We used a constant drive signal for the numerical simulations. Figure 4(a) shows the result of the time series prediction task. In Fig. 4(a), the time series predicted by using the reservoir computing is similar to the input chaotic data. The difference between the two time series is plotted as a prediction error in Fig. 4(b). It is found

that the prediction error occurs when the original chaotic data suddenly decreases in time.

The performance on the task is evaluated by using the normalized mean-square error (NMSE) as follows,

$$NMSE = \frac{1}{L} \sum_{n=1}^L (\bar{y}(n) - y(n))^2 / \text{var}(\bar{y}) \quad (3)$$

where n is the index of the input data and L is the total number of the input data. $y(n)$ is the linear combination of the nodes with trained weights of reservoir computing that are compared to the value $\bar{y}(n)$ as a target data of n -th input data. $\text{var}(\bar{y})$ is the variance of \bar{y} . The NMSE for our prediction task is 0.02 in Fig. 4(b), and this value indicates a good performance of the reservoir computing.

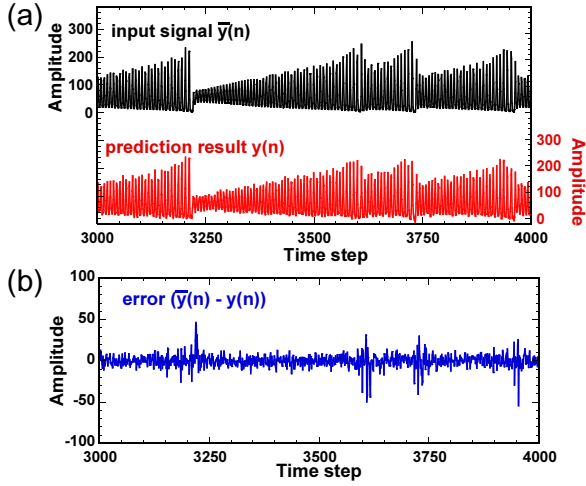


Figure 4: Temporal waveforms of (a) input signal and prediction result, and (b) error signal between them.

3. Performance for chaotic drive input

We used three types of drive signals to improve the performance of Santa Fe time-series prediction task. Figure 5(a) shows the three different drive signal without input signal used for reservoir computing. The first signal is a constant output, denoted as Drive 1 (the black curve in Fig. 5(a)) The second one is a chaotic output generated from a semiconductor laser with optical feedback, denoted as Drive 2 (the red curve). The chaotic signal is generated beforehand and recorded in a memory. The intensity of a constant drive signal is modulated repeatedly by the pre-recorded chaotic signal to generate Drive 2. The bandwidth of Drive 2 is about 7 GHz. We also generate a bandwidth-enhanced chaotic output from two coupled semiconductor lasers, denoted as Drive 3 (blue curve). The bandwidth of the chaotic signal is about 30 GHz. A constant drive signal is modulated by using one of the three types of the drive signals and the input signal with temporal mask.

Figure 5(b) shows the temporal waveforms of the transients of the response laser output. The output of Response i is generated from the input of Drive i ($i = 1, 2, 3$). A square waveform with two binary states are observed in Response 1, corresponding to random modulation of the temporal mask, and transient dynamics are slightly observed at the edge of the square waveform. The temporal waveform of Response 2 is more fluctuated than that of Response 1, since the chaotic drive input is used, instead of the constant drive input. However, the shape of the square waveform still remains. Faster and more complex dynamics are observed in the output of Response 3, where faster chaotic drive input is used. A variety of the chaotic waveforms may result in rich variation of the internal states of the nodes for learning process.

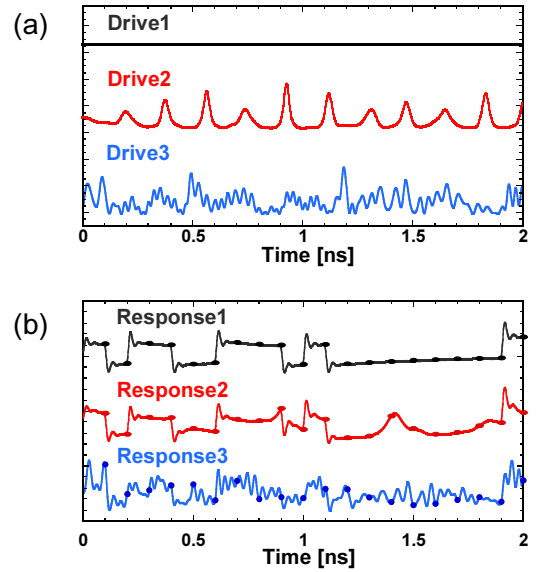


Figure 5: (a) Temporal waveforms of (a) drive and (b) response outputs. Drive1: constant signal, Drive2: chaotic signal, Drive3: bandwidth-enhanced chaotic signal. Response i is generated from Drive i ($i = 1, 2, 3$). The dots indicate the nodes.

Figure 6 shows the performance of the time-series prediction for the three types of the drive signals as the feedback strength κ of the response laser is changed. The NMSE is plotted for the three types of the drive signals. Note that consistency of the response laser is achieved in the range $0 \leq \kappa \leq 82 \text{ ns}^{-1}$. The NMSEs for Drive 1 (the constant signal) and Drive 2 (the chaotic signal) are almost the same values in the consistency region. It is worth noting that the NMSE for Drive 3 (the bandwidth-enhanced chaos) is smaller than those for the Drive 1 and 2 in the consistency region. The performance of the time-series prediction task is improved by using the bandwidth-enhanced chaos. We speculate that the improvement of the performance results from rich dynamics of the response temporal waveforms, as shown in Fig. 5(b).

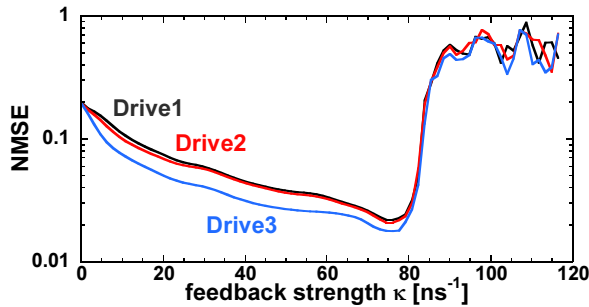


Figure 6: NMSE of the Santa Fe time-series prediction task as a function of the feedback strength κ for three types of the drive signals. $\kappa_{inj} = 155 \text{ ns}^{-1}$.

4. Conclusions

We investigated reservoir computing using consistency of semiconductor lasers with optical feedback and injection by numerical simulations. The performance of the time-series prediction task was carried out. The prediction was succeeded in the region of consistency of the response laser. We also introduced three types of the drive signals: constant, chaotic, and bandwidth-enhanced chaotic signals. We found that the performance of the time-series prediction is improved by using the bandwidth-enhanced chaotic drive signal.

Acknowledgments

We gratefully acknowledge support from a Grant-in-Aid for Young Scientists and Management Expenses Grants from the Ministry of Education, Culture, Sports, Science and Technology in Japan.

References

- [1] H. Jaeger, "The 'echo state' approach to analysing and training recurrent neural networks - with an Erratum note," *GMD Report.*, Vol.148: German National Research Centre for Information Technology, 2001.
- [2] W. Maass, T. Natschläger, and H. Markram, "Real-time computing without stable states: a new framework for neural computations based on perturbations," *Neural Comput.*, Vol. 14, No. 11, pp. 1531, 2002.
- [3] H. Jaeger and H. Haas, "Harnessing nonlinearity: predicting chaotic systems and saving energy in wireless communication," *Science.*, Vol. 304, No. 5667, pp. 78, 2004.
- [4] L. Appeltant, M.C. Soriano, G. Van der Sande, J. Danckaert, S. Massar, J. Dambre, B.Schrauwen, C.R. Mirasso, and I. Fischer, "Information processing using a single dynamical node as complex system," *Nat. Commun.*, Vol. 2, pp. 468, 2011.
- [5] L. Larger, M.C. Soriano, L. Appeltant, J.M. Gutierrez, L. Pesquera, C.R. Mirasso, and I. Fischer, "Photonic information processing beyond Turing: an optoelectronic implementation of reservoir computing," *Opt. Express*, Vol. 20, pp. 3241, 2012.
- [6] Y. Paquot, F. Duport, A. Smerieri, J. Dambre, B. Schrauwen, M. Haelterman, and S. Massar, "Optoelectronic reservoir computing," *Sci. Rep.*, Vol. 2, No. 287, pp. 347, 2012.
- [7] F. Duport, B. Schneider, A. Smerieri, M. Haelterman, and S. Massar, "All-optical reservoir computing," *Opt. Express*, Vol. 20, pp. 22783, 2012.
- [8] D. Brunner, M.C. Soriano, C.R. Mirasso, and I. Fischer, "Parallel photonic information processing at gigabyte per second data rates using transient states," *Nat. Commun.*, No. 4, pp. 1364, 2013.
- [9] K. Hicke, M.A. Escalona-Morán, D. Brunner, M.C. Soriano, I. Fischer, and C.R. Mirasso, "Information processing using transient dynamics of semiconductor lasers subject to delayed feedback," *IEEE J. Quantum Electron.*, Vol. 19, No. 4, pp. 1501610, 2013.
- [10] R.M. Nguimdo, G. Verschaffelt, J. Danckaert, and G. Van der Sande, "Fast photonic information processing using semiconductor lasers with delayed optical feedback: Role of phase dynamics," *Opt. Express*, Vol. 22, No. 7, pp. 8672, 2014.
- [11] A. Uchida, R. McAllister, and R. Roy, "Consistency of nonlinear system response to complex drive signals," *Phys. Rev. Lett.*, Vol. 93, pp. 244102, 2004.
- [12] R. Lang and K. Kobayashi, "External optical feedback effects on semiconductor injection laser properties," *IEEE J. Quantum Electron.*, Vol. 16, pp. 347, 1980.
- [13] Santa Fe time-series prediction
URL: <http://www-psych.stanford.edu/~andreas/Time-Series/SantaFe.html>